Experimental Diaphragm Design for the UTSA Mach 7 Ludwieg Tube

Matt Garcia[1] and Christopher S. Combs[2]
The University of Texas at San Antonio, San Antonio, Texas, 78249, USA

Continued growth and technological advancements in multiple sectors of the aerospace industry have increased the demand for high speed air vehicles. The University of Texas at San Antonio (UTSA) Hypersonics Laboratory has designed and built a Mach 7 Ludwig Tube wind tunnel to research high-speed aerodynamics and compressible flow phenomena. The Ludwieg Tube wind tunnel requires clean flow free of shrapnel for optimal operation. The design of a clean rupturing diaphragm is required to ensure desired flow. The parameters for diaphragm designs are set based on the operating pressures and temperatures of the wind tunnel. Initial testing requires low-pressure diaphragms to burst between the range of 345kPa (50psia) to 1380kPa (200psia) at 273K (536°R) and have fragment-free flow. Aluminum foil diaphragms are used to estimate the thickness required for 3105-aluminum diaphragms to rupture. The testing of 3105-aluminum diaphragms in low-pressure bursts will serve to discover the required thickness to meet initial testing criteria. Aluminum foil diaphragms proved to adequately estimate the thickness needed to rupture 3105-aluminum diaphragms and Schlieren imaging showed fragment-free flow from select diaphragms. Lessons learned from testing will be applied to the design of diaphragms for heated driver tube tests.

I. Introduction

Wind tunnel facilities play a key role in the research and design of next generation hypersonic flight systems. The Ludwieg tube wind tunnel is a type of facility which provides a cost-effective method for high-speed aerodynamic testing. Ludwieg tube facilities can be found in the University of Oxford [1], Air Force Research Laboratory (AFRL) [2], Purdue University [3], Notre Dame [4], the University of Tennessee Space Institute (UTSI) [5], and many more locations worldwide. These facilities were constructed for continued industry and academic research in supersonic and hypersonic flow. The Ludwieg tube functions on the premise of a pressure differential across a nozzle causing supersonic/hypersonic flow at a Mach number designated by the nozzle's area ratio. The driver tube, which functions as the high-pressure chamber, is filled with compressed air and has the option to be heated. Heating of the driver tube is performed to prevent phase change (liquefaction) as the air expands.

Such a wind tunnel can be triggered via a fast-acting valve or by rupturing a single-use diaphragm. Fast-acting valves are reusable and provide mechanically triggered flow. However, fast-acting valves often require custom design and integration into the Ludwig tube facility. These valves may not be a quick solution for initial wind tunnel testing. Burst diaphragms can provide a temporary solution until a fast-acting valve is obtained or be a long-term solution for actuating wind tunnel flow. Diaphragm materials can vary from simple polymer films such as Mylar®, to common metals such as steel, aluminum, and stainless steel [6][7]. Diaphragm material selection is dependent on the wind tunnel's operational characteristics driven by the driver tube pressure, temperature, and gas composition.

AFRL Mach 6 Ludwieg Tube used Mylar®, aluminum and steel diaphragms to actuate the wind tunnel's flow at driver pressures below 2,760kPa (400 psia) [2]. Mylar® diaphragms were ruptured using a melt wire technique that did not always result in complete diaphragm breaks [2]. Aluminum and steel diaphragms were tested in double-diaphragm and single-diaphragm configurations while single-diaphragms had more clean breaks than the double-diaphragm configuration. Single metal diaphragms were pre-scored and ruptured by increasing tunnel pressure [2]. The UTSA Hypersonics Laboratory will not be able to use polymer materials for their Mach 7 Ludwieg tube wind tunnel as the maximum operational pressure and temperature is 13.8MPa (2,000psia) and 427°C (800°F) [6]. These parameters

[1] Graduate Research Assistant, Department of Mechanical Engineering, AIAA Student Member.
[2] Dee Howard Endowed Assistant Professor, Department of Mechanical Engineering, AIAA Senior Member.

must be considered for the terminal objective of providing a clean rupture free of shrapnel, achieving a fully petaled rupture, and conforming to the internal geometry of the tube at any prescribed test pressure and temperature. The design of diaphragms is not unique to the UTSA wind tunnel and is a task performed by several other groups during the startup phase of their facilities. Some detailed diaphragm design processes were given by Van Harberden [7], Henderson [8], and Rast [9]. Key takeaways from these design campaigns were factored into current work.

The initial low-pressure design has required test parameters of achieving a burst between the range of 345kPa (50psia) to 1380kPa (200psia) at room temperature. The materials selected for the initial design are Aluminum foil and Aluminum alloy 3105. These materials were selected based on their mechanical properties, machinability and cost-effectiveness. In the present work 3105-aluminum was scored by a mill and tested under pressure by the driver tube until the maximum allowable test pressure is reached. Schlieren imaging was used to qualitatively visualize the flow quality and check for shrapnel. Results from this effort are presented and discussed in the proceeding section, and a detailed evaluation of the design and manufacturing process will be presented.

II. Diaphragm Manufacturing

The first step in the design and manufacturing process involved creating a template which specifies the bolt pattern and desired score length. The cutout template shown in Fig. 1 was used as a reference when making individual diaphragms to keep features constant. A cross-shaped pattern was chosen to be inscribed in the middle of the diaphragm to provide unique failure points, to serve as a guide for rupture propagation, and obtain the desired 4 petal opening shape upon rupture as shown in Fig 2. The cross-shaped pattern was scribed to different depths and the remaining thickness of each diaphragm was measured.

A. Aluminum Plate Manufacturing

The aluminum alloy 3105 with a thickness of 0.4826mm (0.019in) can be cut into 0.0929m^2 (1ft^2) sections by using a shear press or tin snip scissors. The diaphragms were fixed onto the bed of a manual mill and zeroed out by selecting a corner as a reference point. Bolt holes can be cut by using a hole saw mounted on the mill's spindle using the hole pattern feature on the digital readout. A mill scoring technique was adopted to remove material from the cross-shaped pattern in the 3105-aluminum plate diaphragms by using a stationary rake and three axis movement. The remaining thickness was determined using a digital tabletop caliper. The caliper was modified to measure the grove depth with a thin conical tip. Detail B in Fig. 3 shows a reference for where the remaining thickness is located on a diaphragm. This feature was studied to create trends and understand relationships between the burst pressure. The caliper was placed on a flat level slab of granite to minimize error when setting a reference point of measurement.

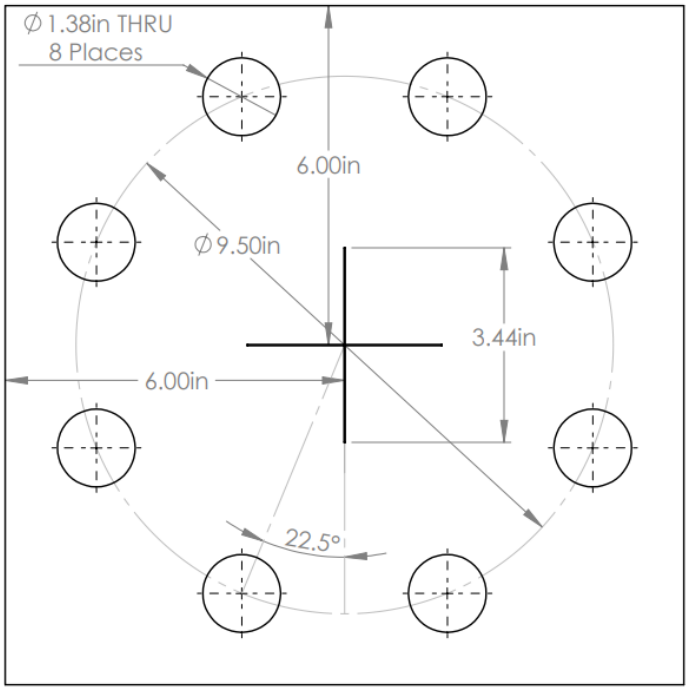

Fig. 1: Diaphragm Cutout Template

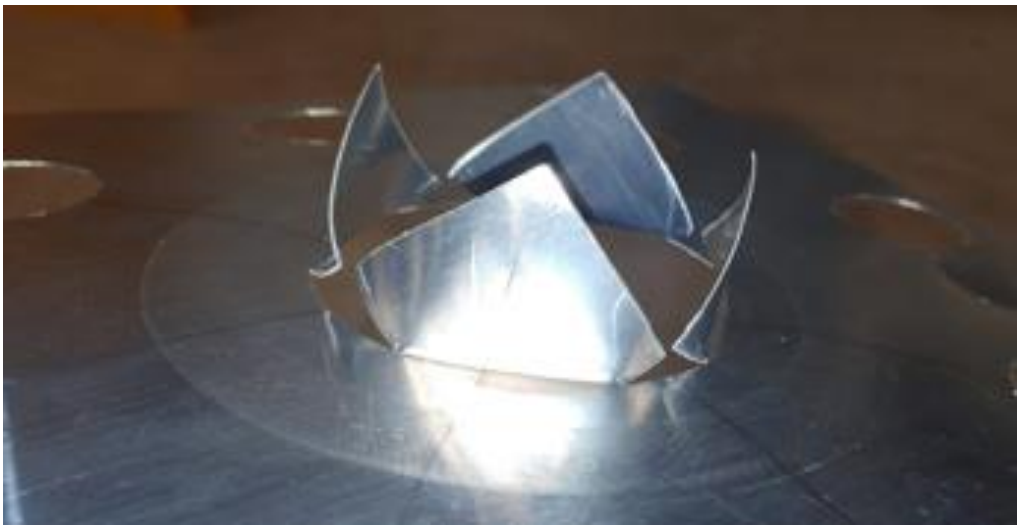

Fig. 2: Fully Petaled Diaphragm

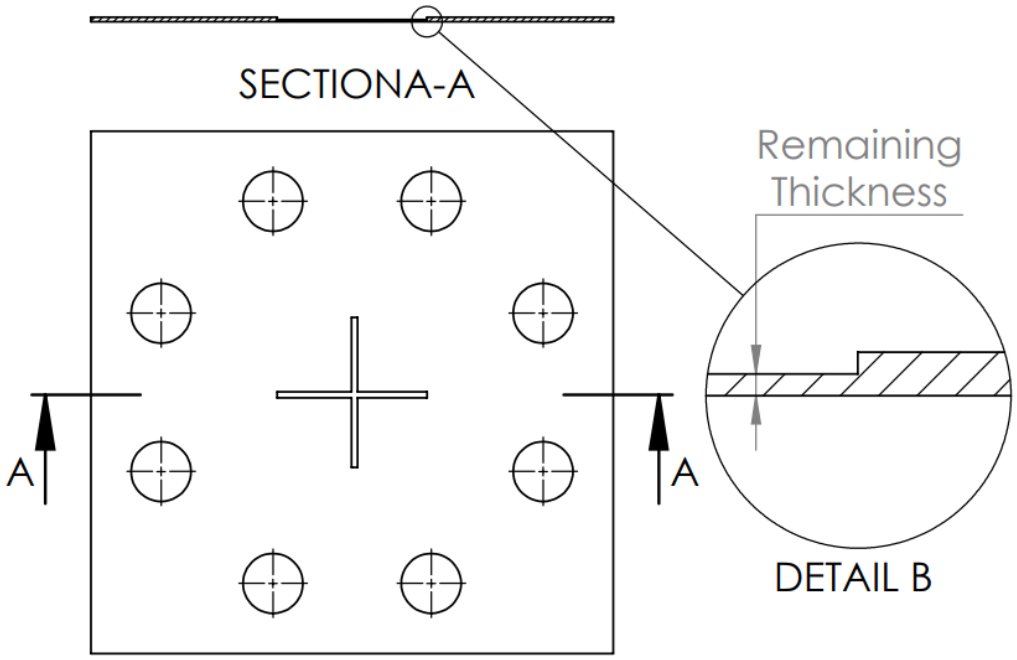

Fig. 3: Reference for Remaining Thickness

B. Aluminum foil Diaphragm Manufacturing

Aluminum foil diaphragms were manufactured to test the scalability of burst pressures with thicknesses. The aluminum foil was manufactured by folding sheets of heavy-duty aluminum foil (~0.0254mm thickness) to the desired thickness and taped to the edges of the gasket. The foil diaphragms did not follow the diaphragm cutout template as it was used only to obtain an estimate for the remaining thickness of the 3105-aluminum and provide a comparison of flow between the two diaphragm types using Schlieren. The final product of both diaphragms can be seen in Fig. 4.

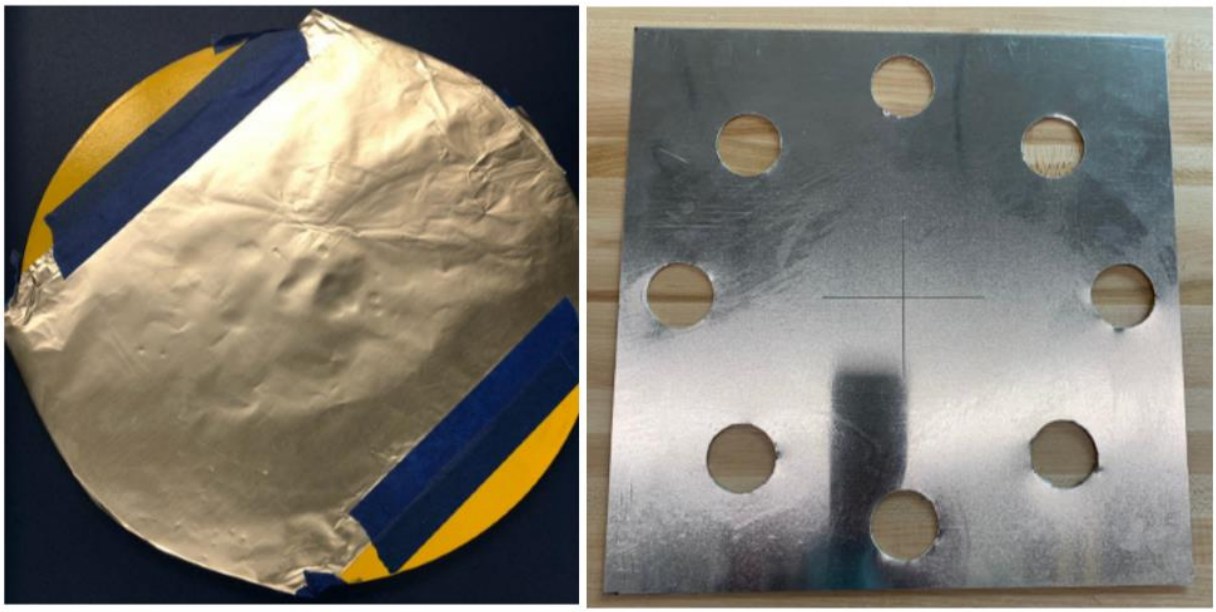

a) **b)**

Fig. 4: Post Manufactured Diaphragms a) Aluminum Foil b) 3105-Aluminum

III. Experimental Considerations

Low-pressure tests were exposed to atmospheric pressure downstream of the bellows and did not involve the use of the low-pressure components (diffuser, nozzle, test section, expansion section, and vacuum tank). A model of the UTSA Mach 7 Ludwieg tube wind tunnel is shown in Fig. 5 to show the low-pressure components within the blue-dashed line while the high-pressure components used for testing are shown within the red-dashed line.

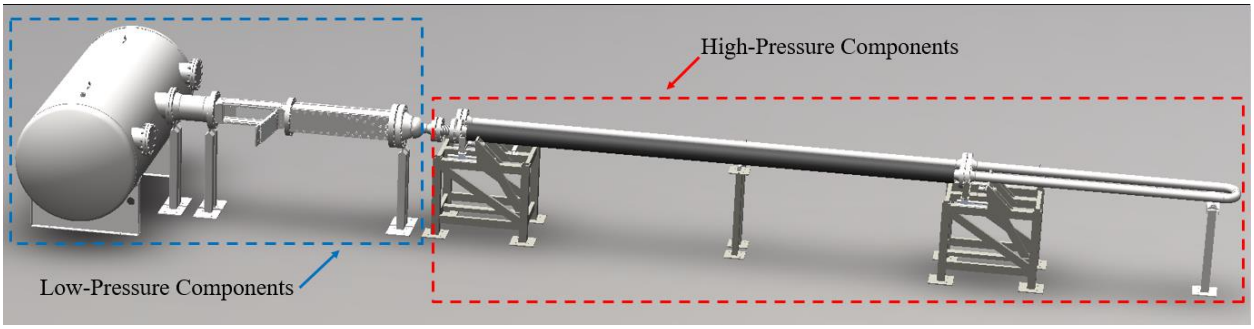

Fig. 5: UTSA Mach 7 Ludwieg Tube Wind Tunnel

The diaphragms were mounted between the bellows and the driver tube flange to set a secure seal along the bore diameter of the flange. A ballistic shield was secured in front of the bellows as a precaution to prevent the spread of diaphragm fragments, if the event were to occur. The placement of diaphragm and ballistic shield can be seen in Fig. 6. A series of 6 Omega PX 319 pressure transducers were used to monitor burst pressures. All pressure data recorded by the pressure transducers were recorded via LabView from the time pressurization began until the chamber reached ambient pressure post-burst. Schlieren images were obtained by using a z-pattern mirror set up shown in Fig. 6 by the yellow light beams. A Photron Fastcam SA-Z was used to acquire images at 20 kHz in order to obtain temporally resolved flow features emanating from the driver tube.

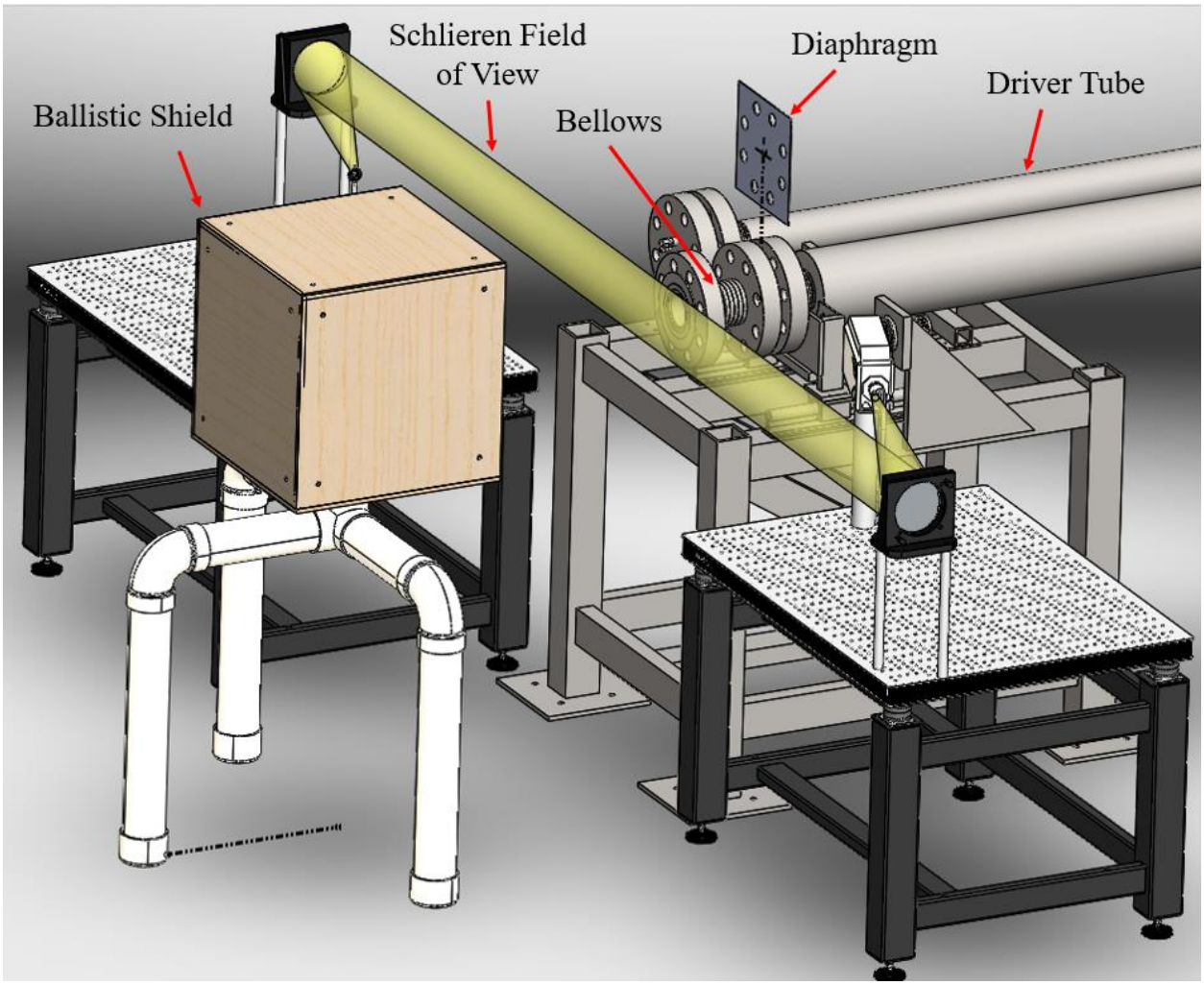

Fig. 6: Experimental Set-Up

IV. Results &Analysis

A. Diaphragm performance (Pressure)

Results obtained from the experimental campaign are detailed in this section. The first results to be presented are those of the aluminum diaphragm tests. In the analysis, the thickness of the aluminum foil was determined by multiplying the number of layers by the thickness of a single sheet. Figure 7 shows the relationship between the thickness of aluminum foil and bust pressure. It can be inferred that the burst pressure rises linearly as the thickness of the foil increases. The 0.1524mm (0.006in) diaphragm which burst at 193kPa (28psia) deviated from the linear trend. Rough handling of this diaphragm created undesired stress points when the foil was folded. Better care and improved quality control processes were adopted once this was revealed.

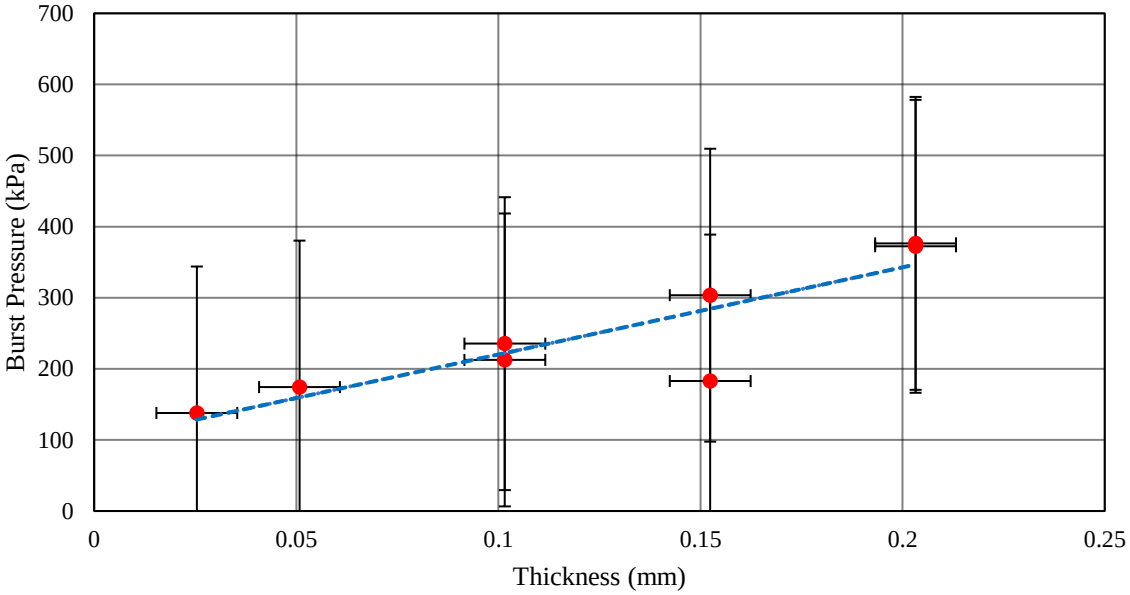

Fig. 7: Aluminum Foil Thickness vs Burst Pressure

The aluminum foil diaphragms were not scored and caused fragments to travel in the flow. Sample images of the single layer aluminum foil diaphragm can be seen in Fig. 8 images a) and b). Fragments of the 8-layer diaphragm seemed to be fused together after rupture and can be seen in Fig. 8 images c) and d). This phenomenon is likely to occur due to the large energy transfer when the diaphragm ruptures. Schlieren images of this phenomenon will be shown in the following sub-section.

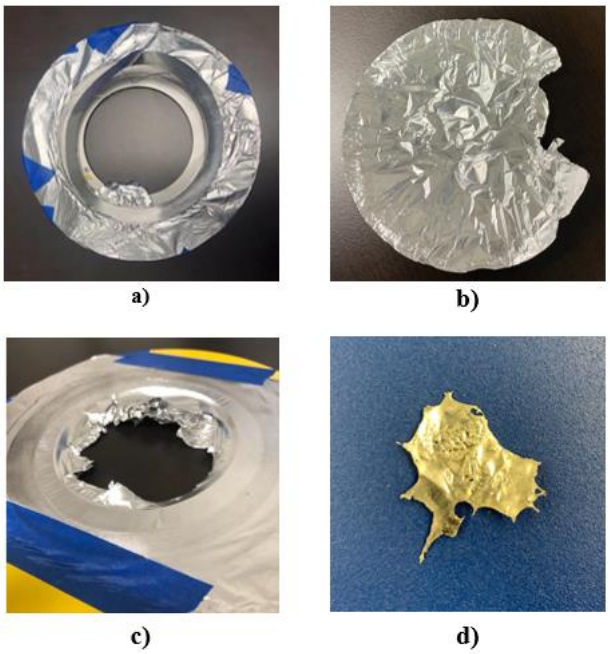

Fig. 8: Post Rupture Aluminum Foil a) & b) 1 Layer Fragmentation c) & d) 8 Layer Fragmentation

The linear trend in Fig. 7 was used to estimate the remaining thickness needed for the 3105-aluminum diaphragms to burst properly for a low-pressure test. The required bust pressure range is between 344.7kPa (50psia) to 1379.9kPa (200psia). Diaphragms for the aluminum alloy 3105 should follow the cut-out template in Fig. 1, and have a remaining thickness, as referenced in Fig. 3, of 0.1524mm (0.006in) or grater to meet the minimum burst pressure requirement.

The burst pressure data for the 3105-aluminum diaphragms can be shown in Fig. 9. The diaphragm with a remaining thickness of 0.254mm (0.01in) and burst pressure of 868.7kPa (126psia) had a fragmented rupture, as seen in Fig 10 images a) and b). This fragmented rupture is considered an outlier as it did not fully petal and adhere to the internal geometry as shown in images c) and d) in Fig. 10.

One of the 0.1524mm (0.006in) diaphragms ruptured at a pressure of 537.7kPa (78psia) while the others ruptured at 303.4kPa (44psia) and 151.7kPa (22psia). This high-pressure irregularity may have been caused when measuring the remaining thickness with the tabletop calipers. All diaphragms, except for the outlier, petaled without releasing fragments. The petaling is seen to adhere to the internal geometry as shown in Fig. 10 image b). Burst pressure in Fig. 9 has a positive liner trend as the remaining thickness increases. This trend has similar characteristics to the trend obtained in the aluminum foil testing. However, they do not obtain the same burst pressure at their varied thickness. This can be due to the initial thickness of 3105-aluminum. The stiffness increases as the initial thickness increases. An increased value in material properties will increase the burst pressure. If the thickness of the material increases the diaphragms will struggle to burst in the required pressure range.

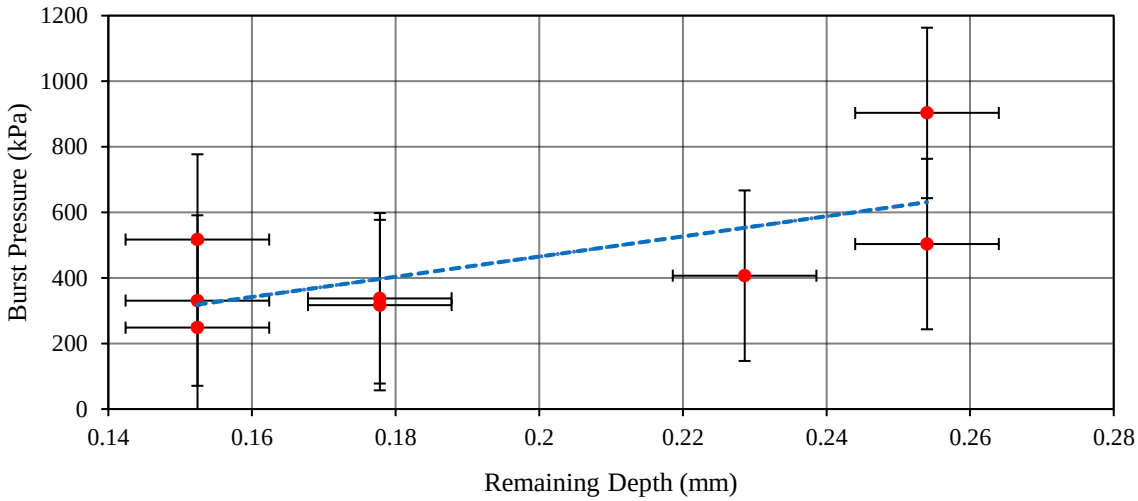

Fig. 9: 3105-Aluminum Remaining Thickness vs Burst pressure

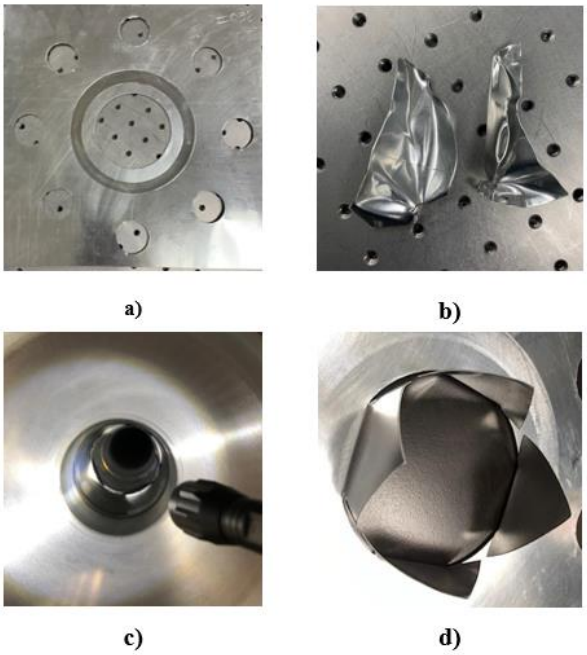

Fig. 10: Post Rupture of 3105-Aluminum a) Fragmented Rupture b) Fully Petaled

B. Diaphragm performance (Flow Quality)

Schlieren imaging was used to qualitatively show the change of flow starting from rupture up to 60ms seconds after burst to verify the quality of flow. This time interval was chosen due to the wind tunnel's run time of 65ms. Each data set was captured with a 20kHz sampling frequency. The following images start from the time interval mentioned above and are divided into 6ms intervals. A background subtraction was performed on all images.

The rupture from a 6 layered aluminum foil diaphragm can be seen in Fig. 11. Images 1 to 3 show the flow when the diaphragm blows out fragmented diaphragm material. The gradients seen in images 4 to 10 show the flow after the fragment has evacuated.

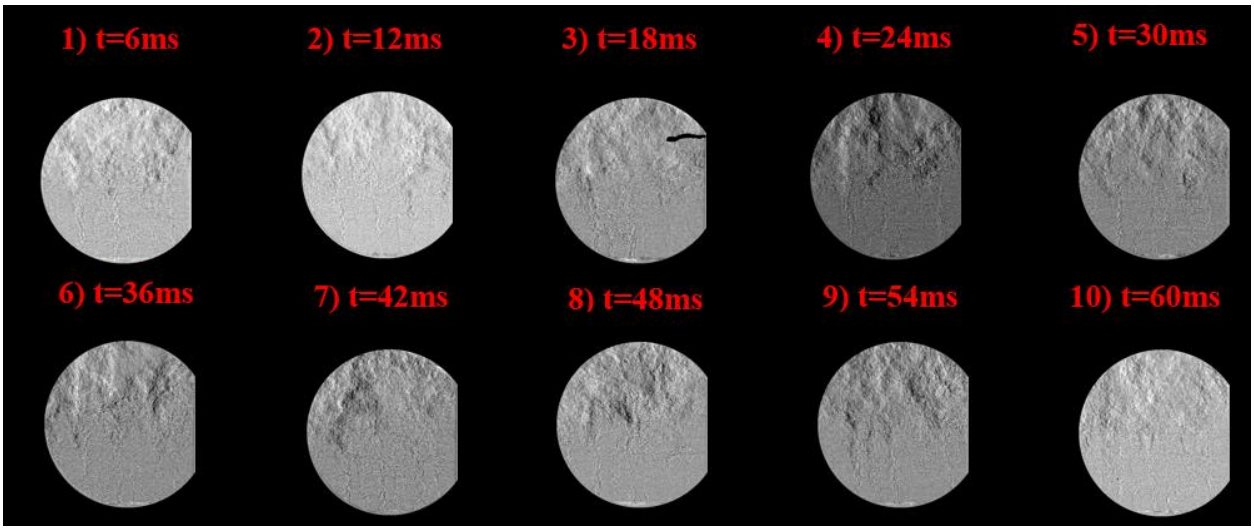

Fig. 11: Schlieren Imaging for Aluminum Foil with 6 Layers

The initial shock wave for a 3105-aluminum with a remaining thickness of 0.228mm (0.009in) can be shown in the first frame of Fig. 12. The shock dissipates through images 2 to 5, while images 6 to 10 show an undisturbed flow as the granular patterns remain consistent. These flow characteristics satisfy the fragment-free flow requirement.

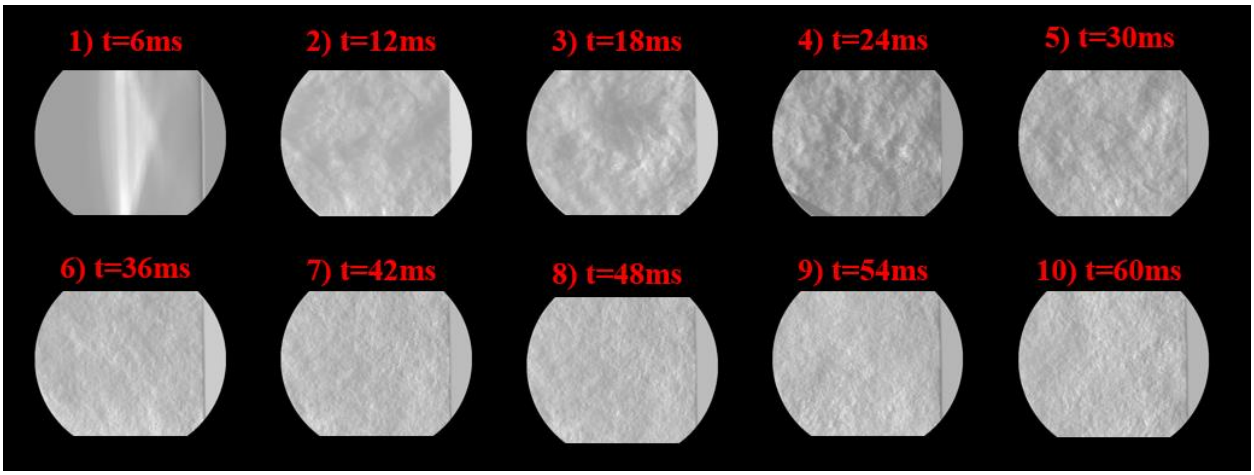

Fig. 12: Schlieren Imaging for 3105-Aluminum Diaphragm with 0.009-inch Remaining Thickness

The 3105-aluminum diaphragm that experienced a fragmented rupture is shown in Fig. 12. Images 1 to 5 show the formation of shockwaves due to the rupture pressure of 951kPa (138psia). Shock angles form as the flow equalizes to ambient pressures. The shock angles shown in Fig. 13 are a common occurrence within nozzles with high pressures relative to ambient pressure. Diaphragm fragments can produce disturbances in the flow and cause an inconsistent flow upstream. Fragmented ruptures, such as the one depicted, can be detrimental for the internal integrity of the nozzle and can damage expensive equipment.

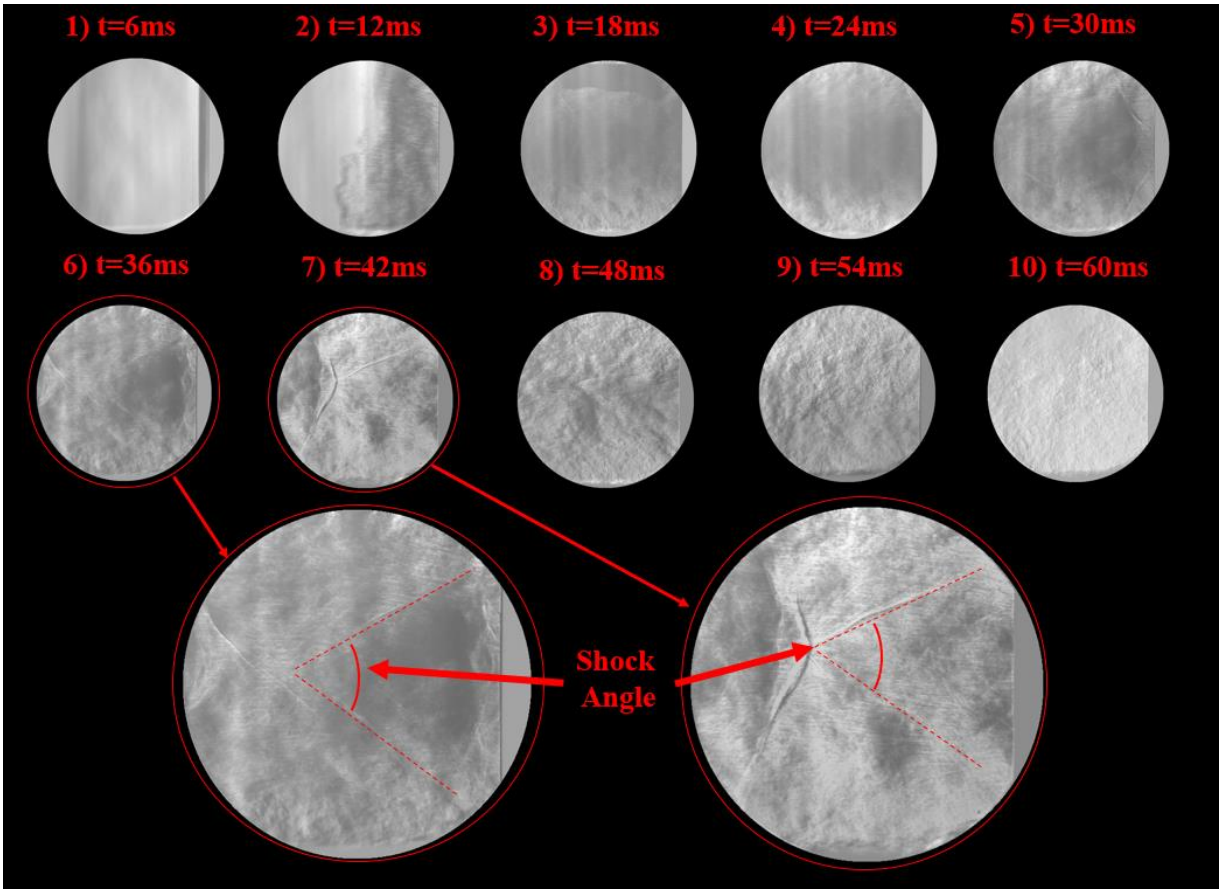

Fig. 13: Schlieren Imaging for 3105-Aluminum Diaphragm Blow-out with 0.01-inch Remaining Thickness

V. Conclusion

An experimental diaphragm design campaign was performed at UTSA to create a standard diaphragm design and manufacturing technique for diaphragms to be used in the new Mach 7 Ludwig tube wind tunnel. This endeavor had to meet the goals of the low-pressure diaphragm requirements. A two-stage process was adopted in this design campaign. The first involved the use of aluminum foil to determine thickness to burst pressure scaling and the second involved the use of 3105-aluminum and a mill scoring technique to manufacture desired diaphragms. The linear trend obtained by bursting the aluminum foil diaphragms provided a range for estimating the remaining thickness needed to burst the 3105-aluminum diaphragms at the low-pressure diaphragm requirements. The 3105-aluminum rupture tests confirm the same linear trend as the aluminum foil. However, the 3105-aluminum ruptured at higher pressures and had a different slope than the aluminum diaphragms. A fragmented rupture occurred with a remaining thickness of 0.254mm (0.01in). This occurrence can be avoided by discarding the use of 3105-aluminum diaphragms with a remaining thickness of 0.254mm (0.01in) or greater. The largest thickness that can satisfy the burst pressure requirements without fragmenting is 0.228mm (0.009in). The flow of the selected diaphragm was compared with the Schlieren images of the aluminum foil and fragmented rupture from the 3105-aluminum test. The aluminum foil had clean flow after the fragments evacuated the bellows. The fragmented 3105-aluminum diaphragm produced shock angles due to high pressures and had disturbed flow due to fragments. In comparison, the selected diaphragm satisfies the fragment-free flow requirements as it did not have any fragments disturbing the flow. The 3105-aluminum diaphragm with a remaining thickness of 0.228mm (0.009in) will be used to initiate the next stage of diaphragm testing. Observations from this campaign will be applied to future tests where this will be expanded to capture burst tests at elevated temperatures and pressures.

Acknowledgments

This work was sponsored (in part) by the Air Force Office of Scientific Research, USAF, under grant/contract number FA9550-20-1-0190. Additional support was provided by NASA grant 80NSSC19M0194. The views and conclusions contained herein are those of the authors and should not be interpreted as necessarily representing the official policies or endorsements, either expressed or implied, of the Air Force Office of Scientific Research, NASA, or the U.S. Government. Funds for wind tunnel construction were also provided by The University of Texas at San Antonio. The authors would also like to thank Eugene Hoffman, Jose Rodriguez, Valeria Delgado, and Elijah LaLonde for helping make diaphragms, creating a virtual interface for data acquisition, and continuously torqueing the flange bolts for each test.

References

[1] Matthew McGilvray, Luke J. Doherty, Andrew J. Neely, Robert Pearce, & Peter Ireland. (n.d.). The Oxford High Density Tunnel. In 20th AIAA International Space Planes and Hypersonic Systems and Technologies Conference.

[2] Roger L. Kimmel, Matthew P. Borg, Joseph S. Jewell, KIng-Yiu Lam, Rodney D. Bowersox, Ravi Srinivasan, Steven Fuchs, & Thomas Mooney. (n.d.). AFRL Ludwieg Tube Initial Performance. In 55th AIAA Aerospace Sciences Meeting.

[3] Juliano, T., Schneider, S., Aradag, S., & Knight, D. (2008). Quiet-Flow Ludwieg Tube for Hypersonic Transition Research. AIAA Journal, 46(7), 1757–1763.

[4] Lakebrink, M., Bowcutt, K., Winfree, T., Huffman, C., & Juliano, T. (2018). Optimization of a Mach-6 Quiet Wind-Tunnel Nozzle. Journal of Spacecraft and Rockets, 55(2), 315–321.

[5] Phillip A. Kreth, Mark Gragston, Kirk Davenport, & John D. Schmisseur. (n.d.). Design and Initial Characterization of the UTSI Mach 4 Ludwieg Tube. In AIAA Scitech 2021 Forum.

[6] Singh, A., Satheesh Kumar, A., & B.T, K. (2020). Experimental investigation of diaphragm material combinations in a small-scale shock tube. Aircraft Engineering and Aerospace Technology, 93(1), 42–50.

[7] Rast, J. J. The design of Flat-Scored High-Pressure Diaphragms For use in Shock Tunnels and Gas Guns. NAVAL ORDNANCE LAB WHITE OAK MD, 1961.

[8] Ian Bashor, Eugene Hoffman, George Gonzalez, & Christopher S. Combs. (n.d.). Design and Preliminary Calibration of the UTSA Mach 7 Hypersonic Ludwieg Tube. In AIAA Aviation 2019 Forum.

[9] Van Harberden, W. (2017). Development of a Supersonic Reflected Shock Tunnel (Unpublished master's thesis). University of Calgary, Calgary, AB. doi:10.11575/PRISM/25676

[10] Henderson, R. W. An Analytical Method for the Design of Scored Rupture Diaphragms for Use in Shock and Gun Tunnels. JOHNS HOPKINS UNIV LAUREL MD APPLIED PHYSICS LAB, 1967.